

Stark effect on the exciton spectra of vertically coupled quantum dots: horizontal field orientation and non-aligned dots

B. Szafran,¹ F.M. Peeters,² and S. Bednarek¹

¹*Faculty of Physics and Applied Computer Science,*

AGH University of Science and Technology, al. Mickiewicza 30, 30-059 Kraków, Poland

²*Departement Fysica, Universiteit Antwerpen, Groenenborgerlaan 171, B-2020 Antwerpen, Belgium*

(Dated: September 1, 2018)

We study the effect of an electric-field on an electron-hole pair in an asymmetric system of vertically coupled self-assembled quantum dots taking into account their non-perfect alignment. We show that the non-perfect alignment does not qualitatively influence the exciton Stark effect for the electric field applied in the growth direction, but can be detected by application of a perpendicular electric field. We demonstrate that the direction of the shift between the axes of non-aligned dots can be detected by rotation of a weak electric field within the plane of confinement. Already for a nearly perfect alignment the two-lowest energy bright exciton states possess antilocked extrema as function of the orientation angle of the horizontal field which appear when the field is parallel to the direction of the shift between the dot centers.

PACS numbers: 73.21.La,71.35-y,71.35.Pq,73.21.Fg

I. INTRODUCTION

The effect of the electric field on the exciton recombination energy is used to probe the properties of the electron and hole confinement in separate self-assembled quantum dots^{1,2} through a strong deformation of the carrier wave functions. For vertically coupled quantum dots³ the electric field oriented in the growth direction leads to a redistribution of the carriers between the dots.^{4,5,6,7,8} Typical electric field applied for vertically coupled quantum dots is of the order of 20-30 kV/cm, i.e., by an order of magnitude smaller than the one used to probe the confinement potential¹ of a single dot. Therefore, such experiments on the electric-field effect for coupled dots resolve rather the properties of the molecular coupling than the fabrication dependent details of the confinement in separate dots. Moreover, the charge redistribution induced by the electric field between the different dots have naturally a much stronger energy effect than deformation of the wave functions inside each of the dots. Due to these features, previous simple modeling⁸ (done in parallel with the experimental work⁴) using a square well vertical and harmonic lateral confinement⁹ led to the correct description of the observed^{4,5} electric field induced dissociation of the electron-hole pair in an avoided crossing of dark and bright energy levels.¹⁰ It also successfully predicted⁸ non-trivial features of the photoluminescence spectrum observed during the negative trion dissociation by the electric field.⁶

A vertical electric field was used very recently⁷ to verify the growth process of intentionally strongly asymmetric double quantum dots. In this paper we demonstrate that the horizontal electric field (perpendicular to the growth direction) can be useful to estimate the non-perfect vertical alignment of the dots and to determine the direction of the horizontal shift between them. To account for the horizontal field effects we replaced the harmonic lateral profile of our previous model⁸ by a quantum well and de-

veloped a computational approach for treating excitons in systems with no axial symmetry and for an arbitrary electric field direction.

The vertical electric field-induced redistribution of charge carriers is smooth only for the electron which tunnels much more effectively between the dots and is responsible for the most characteristic experimental features of the spectrum.^{4,5,6,7,8} Similarly, it is the electron redistribution between the dots due to a rotation of a weak horizontal field that allows for the detection of the non-perfect alignment, the hole charge being only shifted within the separate dots. Therefore, we decided to use for simplicity the single band model to describe the hole.

The paper is organized as follows, Section II describes the computational approach, our numerical results are given in Section III, and Section IV contains the summary and conclusions.

II. DOUBLE DOT MODEL AND METHOD OF CALCULATIONS

We work in the single valence band approximation, for which the Hamiltonian of the electron-hole pair is

$$H = -\frac{\hbar^2}{2m_e}\nabla_e^2 - \frac{\hbar^2}{2m_h}\nabla_h^2 + V_e(\mathbf{r}_e) + V_h(\mathbf{r}_h) - \frac{e^2}{4\pi\epsilon\epsilon_0|\mathbf{r}_e - \mathbf{r}_h|} - e\mathbf{F} \cdot (\mathbf{r}_e - \mathbf{r}_h), \quad (1)$$

with \mathbf{r}_e , \mathbf{r}_h - electron and hole coordinates, m_e , m_h - effective band masses for the electron and the hole, ϵ the dielectric constant, and \mathbf{F} is the electric field. The electron confinement potential of the double dot system is taken in the form of a sum of double disk-shaped quan-

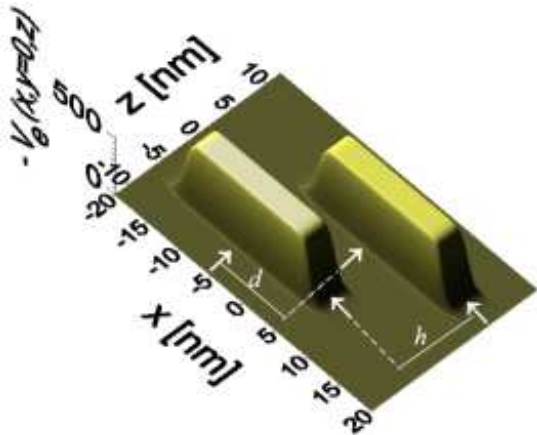


FIG. 1: The electron confinement potential [Eq. (2)] in meV, in the $y = 0$ plane, for the offset between the axes of the dots $d = 10$ nm (equal to the dot radius R) and the vertical distance between the dot centers of $h = 10$ nm. The height of both the dots is $2Z = 4$ nm. The lower (negative z) dot has depth $V_e^l = 518$ meV, the dot for positive z has depth of $V_e^u = 508$ meV.

tum wells with smooth walls (see Fig. 1)

$$V_e(\mathbf{r}) = \begin{aligned} & -V_e^l / \left(1 + \left(\frac{(x-d/2)^2 + y^2}{R^2}\right)^{10}\right) \left(1 + \left(\frac{(z-h/2)^2}{Z^2}\right)^{10}\right) \\ & -V_e^u / \left(1 + \left(\frac{(x+d/2)^2 + y^2}{R^2}\right)^{10}\right) \left(1 + \left(\frac{(z+h/2)^2}{Z^2}\right)^{10}\right), \end{aligned} \quad (2)$$

here R stands for the radius of a single dot, Z is half of its height, the dots centers are placed symmetrically with respect to the origin at points $(x, y, z) = \pm(d/2, 0, h/2)$ (the spacer layer is then equal to $b = h - 2Z$), V_e^l and V_e^u are the lower and upper dot depths, respectively. For simplicity we take the same size of both dots, the inevitable asymmetry between them (due to size difference, indium composition, nonsymmetric strain, etc.) can for the limited purpose of the present paper be effectively taken into account by applying different depths of the dots. The confinement potential for the hole is of the same form, only with depths V_h^l , V_h^u replacing V_e^l and V_e^u . The bottom of the conduction band of the barrier material (GaAs) is taken as the reference energy for electrons, and the top of the GaAs valence band as the reference level for the holes, i.e., the eigenvalues of (1) have to be shifted up by the GaAs band gap to give the photon energy measured in a luminescence experiment.

We previously⁸ demonstrated, that for an interacting electron-hole pair both the energy spectrum and the particle distribution are nearly the same when the asymmetry of the double well is exclusively introduced for one of the particles, since it is translated by the interaction into an asymmetry for the other particle. In this paper we assume that the dot situated on the negative side of the $z = 0$ plane is deeper by 10 meV for both the electron

and the hole $V_e^l = V_e^u + 10$ meV, $V_h^l = V_h^u + 10$ meV, and $V_e^u = 508$ meV, $V_h^u = 218$ meV is taken the same as in our previous paper⁸ assuming that the dots embedded in a pure GaAs matrix are made of $\text{Ga}_x\text{In}_{1-x}\text{As}$ alloy with $x = 0.66$. Accordingly⁸ we take $m_e = 0.037$, $m_h = 0.45$, and $\epsilon = 12.5$. The size parameters are taken from Ref.⁶, diameter $2R = 20$ nm and height $2Z = 4$ nm (therefore $b = h - 4$ nm).

The Schroedinger equation with Hamiltonian (1) is solved using the exact diagonalization (configuration interaction) approach keeping a complete account of the electron-hole correlation. As the basis for the electron-hole pair we take products of single-electron states and single-hole states

$$\phi(\mathbf{r}_e, \mathbf{r}_h) = \sum_{j,k} d_{jk} f_e^{(j)}(\mathbf{r}_e) f_h^{(k)}(\mathbf{r}_h), \quad (3)$$

where $f_e^{(j)}$, $f_h^{(k)}$ are the single-electron and single-hole wave functions of state j and k , respectively. The single-particle wave functions are obtained in the multicenter basis of displaced Gaussian functions,

$$f(r) = \sum_i^M c_i \exp \left[-\alpha_i \left((x - x_i)^2 + (y - y_i)^2 \right) - \beta_i (z - z_i)^2 \right], \quad (4)$$

where c_i are the linear variational parameters, α_i and β_i are the nonlinear variational parameters describing the strength of i -th Gaussian around point (x_i, y_i, z_i) , whose coordinates are variational parameters by themselves. We took 11 basis functions for each of the dots: one situated at the dot center $\pm(d/2, 0, h/2)$, eight around it within the plane of confinement $z_i = \pm h/2$, on a circle with optimized diameter. Two additional centers are placed above and below the center of each dot $\pm(d/2, 0, h/2 + \pm\Delta)$ with Δ optimized variationally. Addition of more centers outside the plane of confinement or including more centers within it does not improve the results significantly. In the configuration basis (3) we include all the single-particle wave functions obtained in a diagonalization of the electron and the hole Hamiltonians each in a basis of form (4) (with position of centers and other nonlinear parameters optimized separately for the electron and hole), which eventually yields 484 *localized* basis functions to treat the exciton. The recombination probability for the exciton state with wave function ϕ is calculated from the envelope wave function as

$$p = \left| \int d^6 \mathbf{r} \phi(\mathbf{r}_e, \mathbf{r}_h) \delta^3(\mathbf{r}_e - \mathbf{r}_h) \right|^2. \quad (5)$$

Two-dimensional version of the multicenter basis was previously used for laterally coupled dots.¹¹ Our study¹² on electron systems in a single circular dot performed with a similar technique showed that the superposition of Gaussians very well approximates the angular momentum eigenstates.

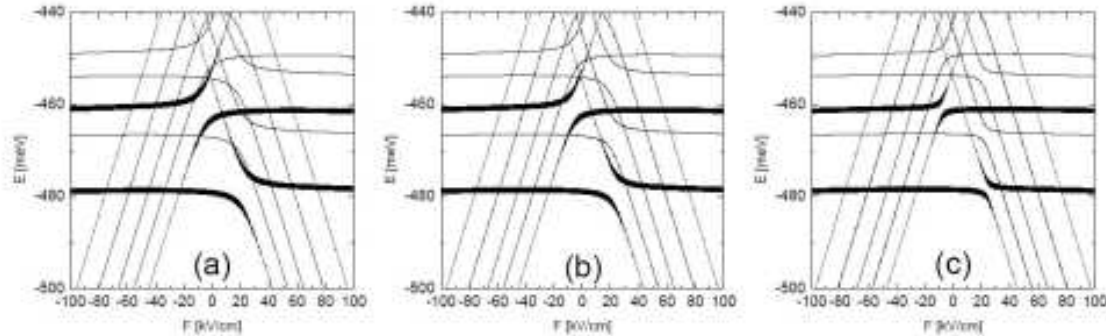


FIG. 2: The exciton spectra for the electric field oriented along the z direction for a vertical distance between the dots centers $h = 10$ nm for (a) perfectly aligned dots $d = 0$, (b) horizontal distance between the vertical symmetry axis of the dots $d = 5$ nm, and $d = 10$ nm (c).

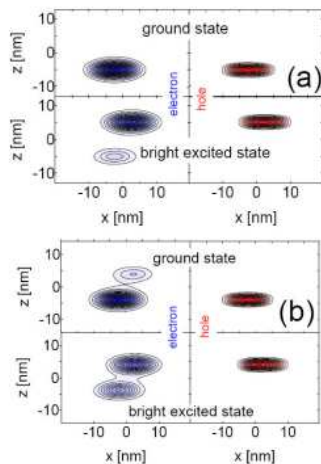


FIG. 3: The electron and hole probability density distributions for the ground state and the first excited bright state in the absence of the electric field for $d = 5$ nm and $h = 10$ nm (a), and $h = 8$ nm (b).

III. RESULTS

The effect of the imperfect alignment of the dots for the exciton Stark effect due to the electric field oriented in the growth direction is presented in Fig. 2. The figure shows the dependence of the exciton spectra on the vertically oriented electric field for the barrier thickness $b = 6$ nm ($h = 10$ nm). For the dots aligned vertically (a) as well as for the offset between the axes of $d = 5$ nm (b) and $d = 10$ nm (c) at $F = 0$ we observe two bright lines (thickness of lines is set proportional to the recombination probability). The particle distribution for the bright states is displayed in Fig. 3. Fig. 3(a) shows the

cross section ($y = 0$) of the electron and hole probability density distributions (obtained through integration of the two-particle probability density in the coordinates of the other particle) for both the bright states at $F = 0$. We notice that in these states the hole is entirely localized in one of the dots, and the electron tends to accompany the hole. In the ground-state the electron is entirely localized in the deeper (lower) dot. In the excited bright state, the electron is predominantly localized in the upper dot, but a small part of the electron wave function leaks to the other (deeper) dot. For thinner spacer layer $b = 4$ nm ($h = 8$ nm) a leakage of the electron density to the dot without the hole appears in the ground state [Fig. 3(b)], and in the excited state it is strengthened. Note, that in the excited state the hole density maximum is displaced to the left within the upper dot following the electron density noticeably shifted to the lower dot.

The vertically oriented electric field $F > 0$ tends to push the electron to the upper (shallower) dot. In the ground state near $F = 20$ kV/cm we see [cf. Fig. 2(a-c)] an avoided crossing of the bright energy level with both carriers in the deeper dot with a dark energy level of separated carriers (hole stays in the lower dot, the electron is transferred to the upper one). The crossing is avoided due to the electron tunnel coupling between the dots. In the upper bright state - no avoided crossing is observed for $F > 0$, the positive electric field stabilizes the electron in the upper dot. On the other hand, for the upper bright energy level, the negative electric field of smaller absolute value (around 10 kV/cm) is enough to transfer the electron from the upper to the lower (deeper) dot which results in an avoided level crossing similar to the one appearing in the ground-state [see the upper avoided crossing at left of $F = 0$ in Fig. 2(a-c)].

We see that for the displaced axes of the dots [Figs. 2 (b-c)] the dependence of the spectra on the vertical elec-

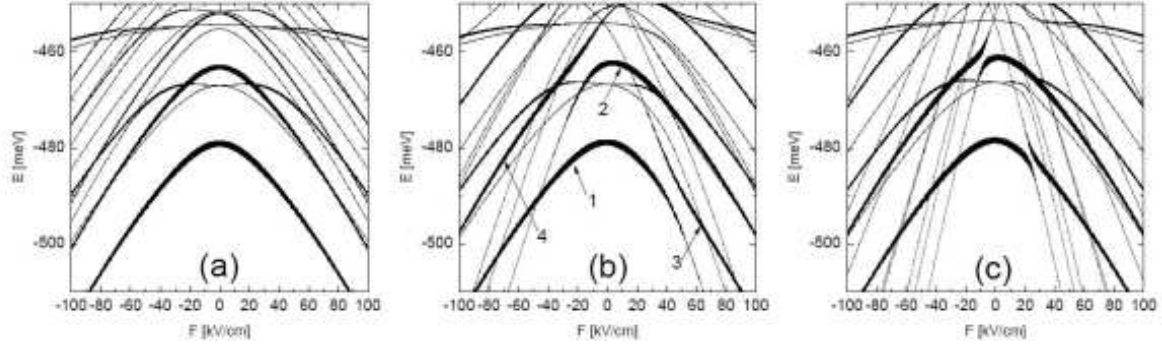


FIG. 4: The exciton spectra for the electric field oriented along the x direction for the vertical distance between the dots centers $h = 10$ nm for (a) perfectly aligned dots $d = 0$, (b) horizontal distance between the vertical symmetry axis of the dots $d = 5$ nm, and (c) $d = 10$ nm. Single-particle densities for the bright energy levels labeled by numbers 1-4 in (b) are presented in Fig. 6.

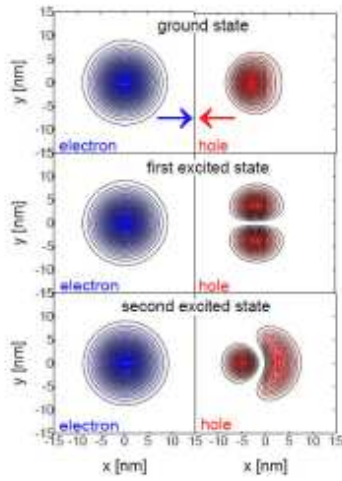


FIG. 5: Electron and hole densities for 3 lowest-energy states for $d=0$ nm and $h = 10$ nm taken within the plane of confinement of the lower, deeper dot ($z = -5$ nm). For the field of $F = 20$ kV/cm parallel to the x axis (arrows at the electron and hole panels at the top-left side of the figure show the direction of the electric force acting on the electron and the hole). The energy levels of these states are displayed in Fig. 4(a).

tric field is qualitatively similar to the perfect alignment case [Fig. 2(a)] but with an avoided level crossings width which is smaller due to the suppressed electron tunnel coupling as the barrier thickness is increased.

Pronounced qualitative differences of the spectra for aligned and not aligned dots appear in case the electric field is oriented horizontally. Fig. 4(a) shows the spectrum for perfectly aligned dots. For both the bright states (with both carriers localized in the same dot) the electric field separates the electron and the hole within each dot pushing the carriers at its opposite sides, which leads to a decreased recombination probability and a de-

creased energy. The first excited state, which is dark and twice degenerated at $F = 0$, corresponds to both carriers in the deeper dot, but with a hole excitation (of p type). The horizontal electric field lifts the degeneracy of the p energy level of the hole. The electron (left panel) and the hole (right panel) density for $F = 20$ kV/cm applied in the x direction is shown in Fig. 5 for the ground-state and the two lowest-energy excited states with p -excitations of the hole. The plot was made in x, y coordinates for the plane of confinement of the lower dot $z = -h/2$ [all the three states correspond to carriers totally localized in the lower dot cf. upper panels of Fig. 3(a)]. The lower dark energy state with p -hole excitation has a nodal surface at the plane $y = 0$, and the parity with respect to this plane is conserved when the field is applied in the x -direction (see the panel of Fig. 5 for the first excited state), hence the zero recombination probability for all F . The other p -level, higher in energy becomes bright at larger F , when the hole parity with respect to the direction perpendicular to the field is destroyed (see the panel of Fig. 5 for the second excited state). We note that in all the three states, for $F = 20$ kV/cm the electron density is not perturbed by the horizontally applied field, but its effect on the hole (for which the confinement is weaker) is clearly visible.

For non-perfectly aligned dots the component of the electric field parallel to the direction of their relative horizontal displacement redistributes the carriers between the dots. The low-energy spectrum plot for $d = 5$ nm (h still equal to 10 nm) contains 4 bright energy levels denoted by 1, 2, 3, and 4 in Fig. 4(b). The modification of the carrier distribution by the electric field in these states is shown in Fig. 6. In the ground state [for $F = 0$ both carriers in the lower dot - see Fig. 3(a)] the electron passes to the right (shallower) dot near $F = +60$ kV/cm. On the other hand, in the excited state which is bright at $F = 0$ and marked by '2' in Fig. 4 both carriers are localized in the upper shallower dot. The electron

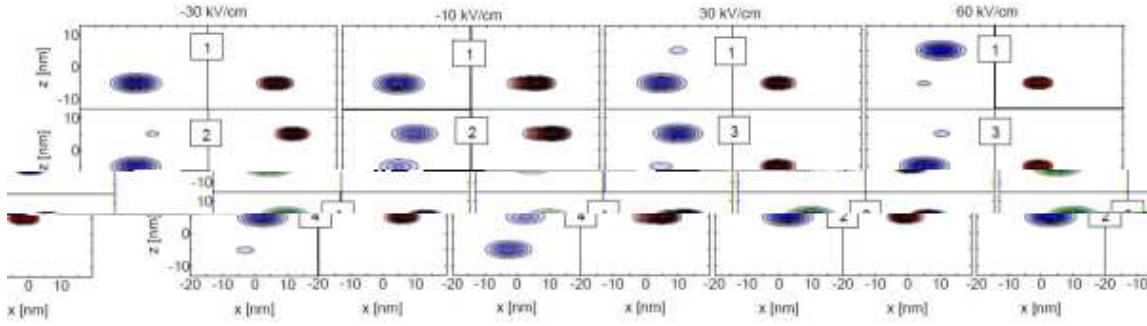


FIG. 6: The $y = 0$ cross section of the electron and hole probability density distributions for the ground state and the first excited bright state for different values of the electric field in the x -direction (given at the top of the figure for each set of plots) for $d = 5$ and $h = 10$ nm. The selected bright states denoted by numbers 1-4, as in Fig. 4(b). The contour plots for states 1 and 2 at $F = 0$ were shown in Fig. 3.

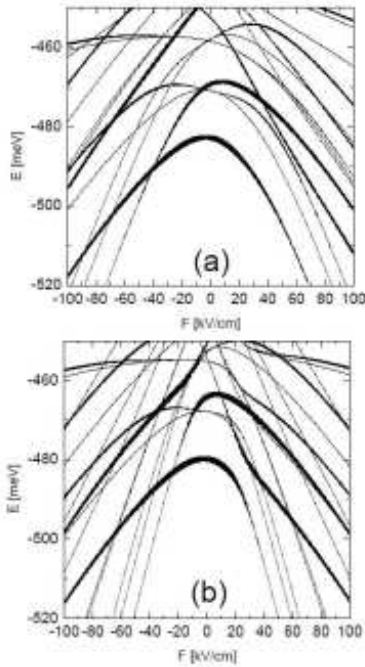


FIG. 7: The exciton spectra for the electric field oriented along the x direction for a vertical distance between the dots centers $h = 8$ nm for (a) horizontal distance between the vertical symmetry axis of the dots $d = 5$ nm. (c) and $d = 10$ nm.

is transferred to the left dot (lower and deeper) for the field around $F = -30$ kV/cm. Both these electron transfers (ground state at $+60$ kV/cm and excited bright state at -30 kV/cm) are associated with avoided crossings of bright and dark energy levels. These avoided crossings become smaller for an offset of 10 nm between the axes of the dots, the case presented in Fig. 4(c).

Fig. 7 shows the spectra for stronger interdot coupling ($h = 8$ nm). Compared to $h = 10$ nm case, the

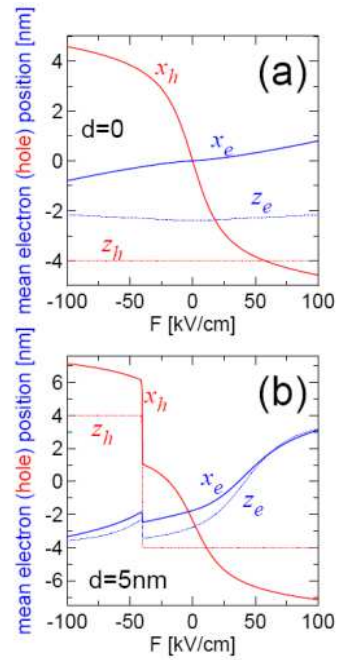


FIG. 8: The ground-state mean electron and hole position dependence on the horizontal electric field oriented along the x direction for $h = 8$ nm (a) perfectly aligned dots and (b) offset of the dots axes of $d = 5$ nm. The energy levels for parameters used in (b) are displayed in Fig. 7(a).

weak-field extrema of the energy levels are shifted more distinctly off the $F = 0$ point due to a larger value of the built-in dipole moment resulting from the shift of the electron density related to the tunnel coupling [see Fig. 3(b) and notice opposite shifts for the extrema of two lowest bright energy levels and much larger value of the dipole moment for the excited state]. The dipole moment ($\mu = |e|(\langle \mathbf{r}_h \rangle - \langle \mathbf{r}_e \rangle)$) is proportional to the difference in the mean positions of the electron and the hole.

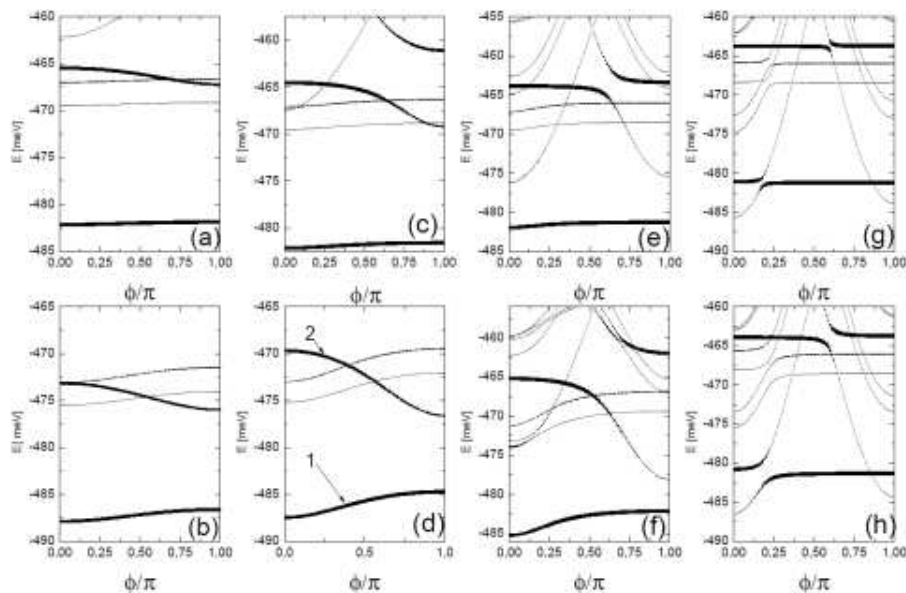


FIG. 9: The exciton spectra for the electric field $F = 20$ kV/cm oriented in the $x - y$ plane as function of the angle between the field and the x axis ($\mathbf{F} = F(\cos(\phi), \sin(\phi), 0)$). The plots in the upper (lower) row correspond to $h = 10$ nm ($h = 8$ nm). Figures (a-b), (c-d), (e-f) and (g-h) correspond to $d = 2, 5, 10$ and 15 nm, respectively. Electron and hole densities for energy levels of plot (d) are displayed in Fig. 10.

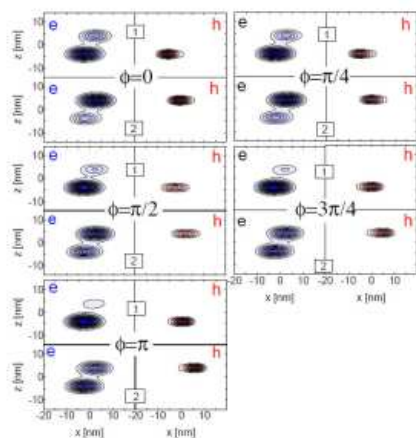


FIG. 10: The $y = 0$ cross section of the electron (the panels marked by 'e') and hole (the panels marked by 'h') probability density distributions for the ground state (denoted by 1 in a square frame) and the first excited bright state (denoted by 2) for $d = 5$ and $h = 8$ nm. The corresponding energy levels are displayed and marked by the same numbers in Fig. 9(d). The horizontal axis corresponds to x variable, the vertical - to z variable. The electric field is kept at $|\mathbf{F}| = 20$ kV/cm, each panel corresponds to a different orientation of the electric field within the $x - y$ plane given by ϕ which is the angle between the \mathbf{F} and the x axis. The left plots in each column show the electron distribution and the right ones—the hole distribution. The plots for states 1 and 2 at $F = 0$ were shown in Fig. 3(b) (ground and excited state, respectively).

The impact of the horizontal field (x) on the spatial position of particles in the ground-state is plotted for $h = 8$ nm in Fig. 8. For perfect alignment $d = 0$ [Fig. 8(a)] the field applied in x direction does not affect the z position of the particles, although one can notice a shallow minimum for the electron at $F = 0$. The horizontal field slightly strengthens the electron confinement within each of the dots thus enhancing the interdot vertical coupling and weakly shifting the electron towards the upper dot. Fig. 8(a) shows a stronger reaction of the horizontal position of the hole than of the electron, which was already noted in the context of Fig. 5. For non-perfect alignment [$d = 5$ nm, see Fig. 8(b)] the horizontal field (x) leads to a very strong dependence of the vertical positions (z) of the particles. For $F > 0$ the electron is transferred to the dot at right and is shifted to the top while hole is stabilized in the left dot. Due to the electron tunnel coupling the electron position is continuous and a smooth function of F . On the contrary the ground-state values of the hole position have a strong jump at $F < -40$ kV/cm, where the crossing of energy levels appear in the ground-state [cf. Fig. 7(a)]. Note that also the electron positions are modified during this jump - the electron, localized in the lower (left) dot tends to follow the hole when it leaves to the upper (right) one.

Fig. 9 shows the low-energy exciton spectrum for a fixed, rather small, length of the electric field of $F = 20$ kV/cm as function of the angle ϕ that it forms with the x axis, $\mathbf{F} = F(\cos(\phi), \sin(\phi), 0)$. The upper panel of the figure corresponds to $h = 10$ nm and the lower to $h = 8$ nm. The plots from left to right are calculated for off-

sets $d = 2, 5, 10$ and 15 nm (for perfectly aligned dots $d = 0$ the spectra are independent of ϕ). Already for the smallest offset [Figs. 9 (a-b)] we notice that the ground state energy is minimal when the field is oriented to the right ($\phi = 0$), i.e., when it tends to transfer the electron to the shallower right dot, and maximal when the field is oriented to the left (tends to keep the electron in the deeper – left dot). For the excited bright state (when both carriers tend to remain in the shallower – right dot), the energy is maximal when the field pushes the electron to the right (reduced penetration of the electron to the other - deeper dot) and minimal in the opposite case (enhanced tunneling to the other dot). The energy dependence of the excited bright state on ϕ is stronger than for the ground state. This is due to the larger electron tunnel coupling for the excited state [see Fig. 3]. The electron is simply more willing to pass to the deeper dot.

For a larger offset of $d = 5$ nm [Fig. 9(c-d)] the dependencies of the bright energy levels on the angle ϕ preserve their character but become more pronounced. The electron and hole densities in the $y = 0$ plane are plotted in Fig. 10 for the two lowest-energy bright energy levels of Fig. 9(d) and for opposite field orientation. They are to be compared to the $F = 0$ case displayed in Fig. 3(b), which shows that in the absence of the field the probability to find the electron in the upper dot for the ground state was smaller than the probability to find the electron in the lower one in the excited bright state. Field of 20 kV/cm at $\phi = 0$ (F oriented in x direction) reverses this relation, as the field shifts more of the electron to the upper dot when in the ground state and removes the electron from the lower dot when in the excited state. A shift of the hole distributions to the left and the squeeze of the distribution to the left side of the dot is also visible. For the electric field oriented along the y direction ($\phi = \pi/2$) the electron distribution of the carriers between the dots is similar to the $F = 0$ case. For the field oriented antiparallel to the x axis ($\phi = \pi$) the electron is almost entirely localized in the left dot when in the ground state and almost completely so when in excited state.

The anti-locking of the energy extrema as function of ϕ for the two lowest bright states observed in Figs. 9 (a-d) at the electric field orientation matching the direction of the shift between the dots can be explained in the following way. The electric field leads to a decrease of the energy levels through the separation of the electron and hole charges [see Eq. (1)]. In the ground state [see Fig. 10] the field at the angle $\phi = 0$ ($+x$ direc-

tion) enhances the separation stimulating the electron to leave the hole [hence the energy minimum see Fig. 9(d)], and at $\phi = \pi$ ($-x$ direction) prevents the electron-hole separation (hence the maximum). In the excited bright state the effect of the field on the carrier separation is opposite. For the excited state the modulation of the recombination probability is more pronounced, the electron coupling and the electron switching between the dots is stronger, hence the more pronounced energy dependence on ϕ [Fig. 9(d)].

For the offset of dot axes equal to the radii $d = 10$ nm – Figs. 9(e-f) the excited bright energy level is involved in an avoided crossing with a dark energy level. For even larger offset $d = 15$ nm – Figs. 9(g-h) an avoided crossing appears also in the ground state. The appearance of these anticrossings is due to the stronger energetic effect of constant F for increased d .

IV. SUMMARY AND CONCLUSIONS

In summary, we have shown that for vertically coupled dots their non-perfect alignment does not qualitatively influence the exciton Stark effect of the electric field oriented in the growth direction. Although for perfectly aligned dots the horizontal electric field only deforms the electron and hole density within each of the dots, for non-perfect alignment it leads to a redistribution of the particles between the dots, i.e., in the direction perpendicular to the field. We demonstrated that due to the relatively strong electron tunnel coupling and strong electron confinement within each of the dots the horizontal electric field can be used to tune the electron distribution in the vertical direction only weakly affecting the electron charge distribution within each of the dots. On the other hand, due to a weaker hole confinement the horizontal field distinctly affects the hole distribution within each of the dots, and the hole transfer between the dots is rapid due to negligible tunnel coupling. We have shown that a rotation of the electric field vector within the plane of confinement can be used to detect the non-perfect alignment. To determine the direction of the horizontal shift between the non-aligned dots, and to estimate the length of the shift, they can be observed from the exciton photoluminescence spectrum.

Acknowledgments This work was supported by the EU network of excellence SANDiE, the Belgian Science Policy and the Foundation for Polish Science (FNP).

¹ P.W. Fry, I.E. Itskevich, D.J. Mowbray, M.S. Skolnick, J.J. Finley, J.A. Barker, E.P. O'Reilly, L.R. Wilson, I.A. Larkin, P.A. Maksym, M. Hopkinson, M. Al-Khafaji, J.P.R. David, A.G. Cullis, G. Hill, and J.C. Clark, Phys. Rev. Lett. **84**, 733 (2000).

² J.A. Barker and E.P. O'Reilly, Phys. Rev. B **61**, 13840

(2000).

³ Q. Xie, A. Madhukar, P. Chen, and N.P. Kobayashi, Phys. Rev. Lett. **75**, 2452 (1995).

⁴ H.J. Krenner, M. Sabahtil, E.C. Clark, A. Kress, D. Schuh, M. Bichler, G. Absteiter, and J.J. Finley, Phys. Rev. Lett. **94**, 057492 (2005).

- ⁵ E.A. Stinaff, M. Scheibner, A.S. Bracker, I.V. Pomonarev, V.L. Korenev, M.E. Ware, M.F. Doty, T.L. Reinecke, and D. Gammon, *Science* **311**, 636 (2005).
- ⁶ H.J. Krenner, E.C. Clark, T. Nakaoka, M. Bichler, C. Scheurer, G. Absteiter, and J.J. Finley, *Phys. Rev. Lett.* **97**, 076403 (2006).
- ⁷ A.S. Bracker, M. Scheibner, M.F. Doty, E.A. Stinaff, I.V. Pomonarev, J.C. Kim, L.J. Whitman, T.L. Reinecke, and D. Gammon, cond-mat/0609147, *Appl. Phys. Lett.* in print.
- ⁸ B. Szafran, T. Chwiej, F. M. Peeters, S. Bednarek, J. Adamowski, and B. Partoens, *Phys. Rev. B* **71**, 205316 (2005).
- ⁹ Similar potential model was also used for the magnetic-field related avoided-crossings by Y.B. Lyanda-Geller, T.L. Reinecke, and M. Bayer, *Phys. Rev. B* **69**, R161308 (2004) as well as in a work for exciton complexes in the in-plane magnetic field by D. Bellucci, F. Troiani, G. Goldoni and E. Molinari, *Phys. Rev. B* **70**, 205332 (2004).
- ¹⁰ For a previous theoretical view on the Stark effect in vertically coupled dots see W. Sheng and J-P. Leburton, *Phys. Rev. Lett.* **88**, 167401 (2002); K.L. Janssens, B. Partoens, and F.M. Peeters, *Phys. Rev. B* **65**, 233301 (2002). A couple of theoretical papers on the exciton dissociation by the electric field with results qualitatively identical to Ref.⁸ have appeared very recently, cf. W. Chu and J.L. Zhu, *Appl. Phys. Lett.* **89**, 053122 (2006) and M.H. Degani, G.A. Farias, and P.F. Farinas, *Appl. Phys. Lett.* **89**, 152109 (2006).
- ¹¹ B. Szafran, F. M. Peeters, and S. Bednarek, *Phys. Rev. B* **70**, 205318 (2004).
- ¹² B. Szafran, F. M. Peeters, S. Bednarek, and J. Adamowski, *Phys. Rev. B* **69**, 125344 (2004).